Influence of Planet Carrier Misalignments on the Operational Behavior of Planetary Gearboxes

Prof. Dr.-Ing. Christian Brecher, Dr.-Ing. Dipl.-Wirt.-Ing. Christoph Löpenhaus and Julian Theling M.Sc.

Introduction and Motivation

The measurement results as well as the analysis of the present paper have been generated in the context of a project funded by the Federal Ministry of Economic Affairs and Energy (BMWi) with the title "Loads on the drive components of wind turbines" (FKZ 0325799). The main objective of the project is the further improvement of the validity of today's simulation models by means of the first large-scale validation by means of a wind turbine. In the long term, this should enable the systematic optimization of the function and reliability of the electromechanical drive-train of wind turbines (Ref. 2).

The test object is a 2.7 MW wind turbine modified in cooperation with the project partners, cf. (Fig. 1). It is driven via a 4 MW direct drive, which provides a maximum torque of 3.4 MNm starting at a rotational speed of 4 rpm, thus eliminating the need for an additional gearbox on the input side. A non-torque load unit (NTL) is installed next to the drive motor. This enables the test nacelle to be loaded in the remaining five degrees of freedom. Thus, it is possible to simulate bending moments and forces of external wind loads and to apply them to the test drive train even in dynamic conditions. The gearbox has the same design and macro geometry as a Winergy wind turbine gearbox. The micro geometry of the gears was redesigned so that all geometry parameters of the gears are known (Ref. 3).

One sub objective of the project is to identify the influence of external loads caused by the wind-field and electrical grid on the loading of drive train components. External loads caused by different wind conditions result into bending moments and forces on the input shaft of the nacelle, which lead to deformations and misalignments in the gearbox. The input forces and bending moments can be simulated aerodynamically and applied on the input shaft by means of the NTL.

In the test gearbox consisting out of a planetary gear stage and two cylindrical gear stages approximately 150 sensors are applied, in order to measure for example the misalignment and the effect of the misalignment on the component loading. Therefore, position sensors as well as strain gauges in the tooth root of the sun and ring gear are applied. Furthermore, the rotational position of every shaft as well as the deviation of the whole housing are measured.

Shaft Misalignments in Cylindrical and Planetary Gearboxes

Similar to cylindrical gears, shaft misalignments in planetary gearboxes result amongst other influences from manufacturing tolerances and load-dependent deformations of the shaft-bearing system. The loads that lead to this deformation can be either external loads from surrounding elements or internal loads resulting out of the radial, axial and tangential components of the gear mesh forces. Due to the trend towards higher power densities, the internal loads increase, while at the same time thinner and thus generally less stiff surrounding structures are used (Ref. 9). As a result, higher deformations and thus also higher shaft misalignments are to be expected in the future.

Shaft misalignments always occur when the rotary axes of one or more gears deviate from the ideal position e.g. due to deformation or assembly tolerances, cf. (Fig. 2). A distinction can be made between parallel displacements of the axes, which result in a center distance deviation and angular misalignments. Regarding involute gears, the effect of angular misalignments is typically more important. Angular misalignments can be distinguished in terms of inclination and skew. An axis skew corresponds to a rotation of the axis in relation to each other about the axes connecting line. An axis inclination exists when the axes of the gears are rotated in the plane defined by those axes in misaligned condition

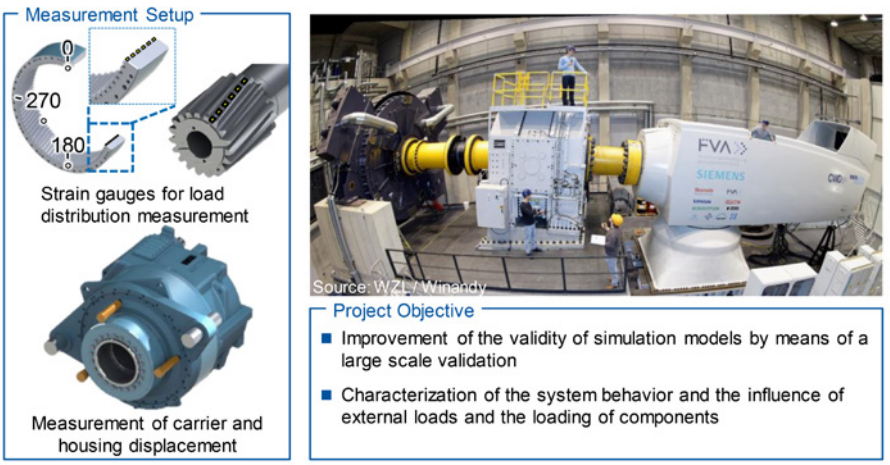

Figure 1 Test setup and objective. © WZL

This paper was first presented at the 8th WZL Gear Conference in the USA July 23/24, 2019.

and thus intersect each other. According to Wittke, both components of angular misalignments can be summed up into a resulting lead angle deviation $f_{H\beta}$ (Ref. 16). The lead angle deviation can be calculated by means of the pressure angle at the operating pitch diameter α_{wt} as well as the inclination or skew angle (Ref. 16).

The misalignments occurring with cylindrical gears can in principle be transferred to planetary gears. Due to the existing kinematics and the loads of the individual elements, other types of misalignment can occur which can also have different local effects on the gear mesh (Ref. 11).

Simple planetary gearboxes consist of the central elements sun gear, ring gear and planet carrier, as well as usually three or more planets (Fig. 2). Due to the arrangement, each gear has several meshes. The load on the surroundings, i.e. — the shafts, bearings and carriers, results from the superposition of the gear loads from the individual meshes. The sun gear is often mounted in an adjustable manner via a spline-tooth coupling or spherical roller bearing in order to find an ideal position for itself on the basis of the individual force components. The aim is to transfer the load as evenly as possible to all planets. A displacement is therefore intended and desired at the sun wheel (Ref. 1). Ring gears are mainly designed as housing elements; misalignment of the ring gear is therefore strongly dependent on the misalignment of the housing (Ref. 13).

The planet gear is in contact with the ring and sun gear. The tangential tooth forces of the planet point in the same direction due to the flank change and have the same magnitude due to the torque compensation and the equal base diameter. In the case of helical gears, in addition to radial and tangential forces, axial forces also occur. In the ring gear mesh and sun gear mesh of the planet, the axial forces are directed in the opposite direction and balance each other out. The force acting points of the two meshes are located in different areas of the planet, as a result of which an axial bending moment is applied. This must be balanced by the planet bearing and the planet pin.

The planet carrier has a significant influence on the deformation within planetary gearboxes. The tangential forces of the individual planetary gears are supported at the carrier and thus generate the carrier torque (Ref. 15). Due to the one-sided torque transmission at the carrier shaft, the torsional moment varies in magnitude over the face width. Furthermore, the carrier wall facing away from the carrier shaft has a lower torsional stiffness due to the bar-shaped connection. The effect is a twisting of the two carrier walls in relation to each other and thus a misalignment of the planet shaft mounted in the carrier walls. Like the planets, the carrier is free of radial and axial forces. An additional displacement of the carrier caused by mesh forces is therefore unlikely. External loads such as the weight force or forces acting from

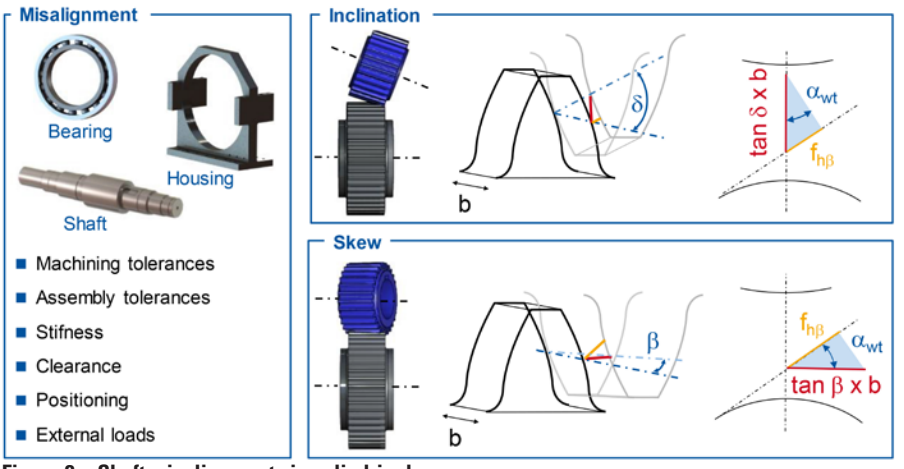

Figure 2 Shaft misalignments in cylindrical gears.

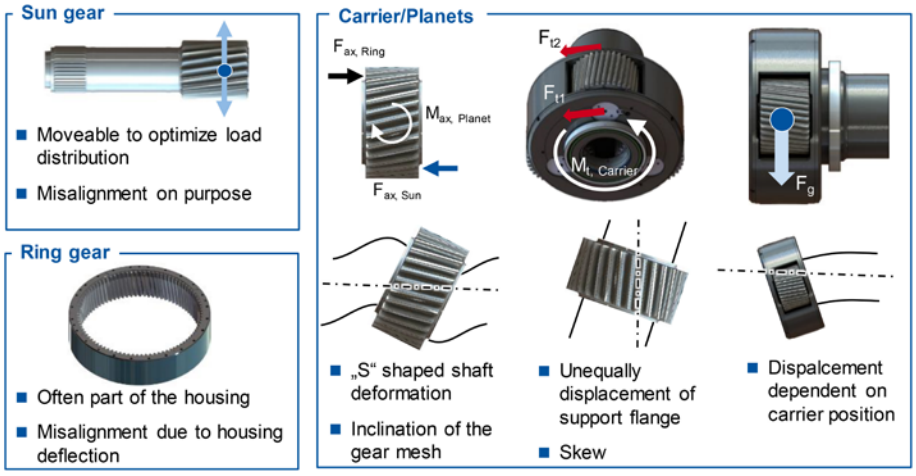

Figure 3 Misalignments in planetary gear stages. © WZL

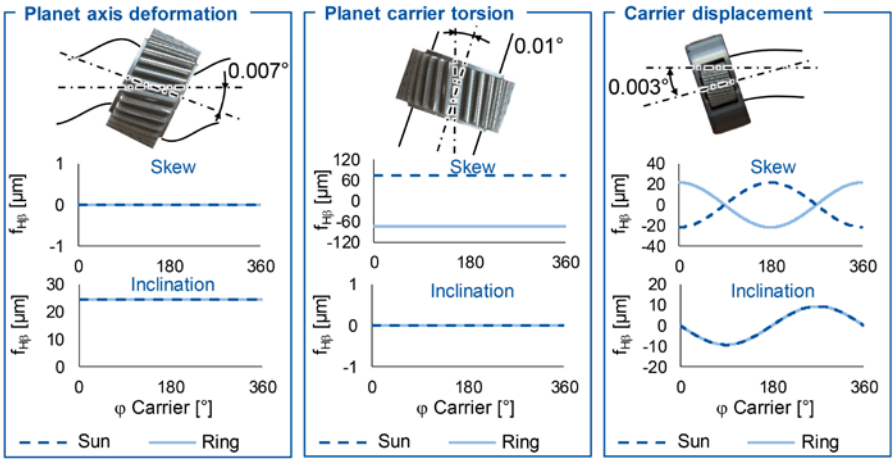

Figure 4 Effect of misalignments on the gear mesh conditions. © WZL

connecting components of the carrier shaft, such as rotors in wind turbines, are therefore the main cause of misalignment. Other influencing factors are bearing clearance and tolerances as well as manufacturing and assembly deviations.

In Figure 4 the effect of the different misalignments on the resulting lead angle deviation and therefore meshing conditions is presented. Therefore, tolerances of the shaft-hub connections are analyzed and transformed into a resulting lead angle deviation according to Wittke (Ref. 16). The selected displacements represent the characteristic displacements of planetary gears: "S-Shape" due to the bending moment of the axial forces on the planet; planetary displacements due to different twisting of the carrier walls and a misalignment of the carrier due to external loads or misalignment of the housing.

The planetary axis misalignment due to axial forces of the planet causes a pure inclination of the planet, since the axis of rotation of the tilting is perpendicular to the axis connection line of sun and planet (Fig. 4); the carrier position shows no influence.

A similar effect is caused by the planetary displacement due to a different twisting of the carrier walls. The displacement takes place in the tangential direction. In contrast to the planetary axis misalignment, a pure skew is present; there is also no dependence on the carrier position. Due to the mathematical transformation of the angular misalignment on the gear mesh via the sine of the pressure angle at inclination and the cosine at skew, the skew has a bigger influence for the same angular misalignment.

Carrier misalignments result in a component of inclination and skew. The inclination and skew curves are phase-shifted by exactly a quarter rotation of the carrier. Due to the different influence of inclination and skew on the gear mesh, the resulting lead angle deviation is not constant. Planet carrier misalignments are comparable to a wobble in cylindrical gears. The amplitude of the lead angle deviation depends on the rotation angle of the carrier. For the carrier positions 90° and 270°, there are only inclination effects — for 0° or 360° and 180° only skew.

Objective and Approach

The objective of this report is to describe the effects caused by misalignments in planetary gearboxes and take them into account during the optimization and design process. Therefore, measurement data of the FVA nacelle has to be evaluated with respect to misalignments and their influence on the loading of the gears. In order to achieve a balanced design, both the load on the tooth flanks and the excitation behavior have to be included in the design process. In order to achieve the objective, four sub-objectives have to be fulfilled (Fig. 5.)

In order to regard the misalignments in the tooth contact analysis, the FE-based tooth contact analysis *FE-Stirnradkette* is extended in order to depict a complete tooth hunt of a planetary gear stage and take into account time-variable misalignments. This is necessary because the effect of a carrier misalignment has different influences on the mesh, depending on the current position. The extension is validated afterwards by a comparison between the calculated tooth bending stress and the measured stresses.

To evaluate the excitation behavior, the transmission error of a complete tooth hunt is calculated as a sequence of individual pitches. The resulting time signal is transferred to the frequency domain and the effects are analyzed. Subsequently, a method to calculate local damage is developed, which considers the variable mesh positions in combination with the angular positions of the elements in planetary gearboxes.

At the end, the tooth flank has to be optimized in order to achieve less damage and a lower noise excitation with the aid of derived characteristic values. Therefore, an approach is used which is based on characteristic values derived in the first work packages that are input variables of a variant calculation carried out with the *FE-Stirnradkette* in combination with the statistical evaluation software *µOpt* to ensure a balanced and robust design against additional misalignments.

The input stage of the wind turbine gearbox of the FVA nacelle is selected as the application case for investigating the influence of misal- ignments in planetary gear stages. Besides the fact that the geometry is known, a further reason for the choice of the demonstrator is the existence of numerous test results. In particular, the misalignments of the planet carrier in relation to the housing are known for numerous load situations with loads in all six degrees of freedom. Selected test points together with the corresponding measured carrier misalignment represent the investigated operating points.

Description of Contact Conditions in Misaligned Planetary Gearboxes

The first sub-objective is the description of the contact conditions for misaligned planetary gearboxes. First, a method is developed which converts the shaft misalignment to the mesh according to the Wittke method as shown (Fig. 4) (Ref. 16). A main challenge is the consideration of the position-dependent carrier misalignment. The mesh specification is then used as input for the FE-based tooth contact analysis. Subsequently, measurement results of the FVA nacelle are presented and essential effects are described. The measurement is then compared to the simulation to validate the method.

Extension of the FE-Stirnradkette. In the following section, a method is

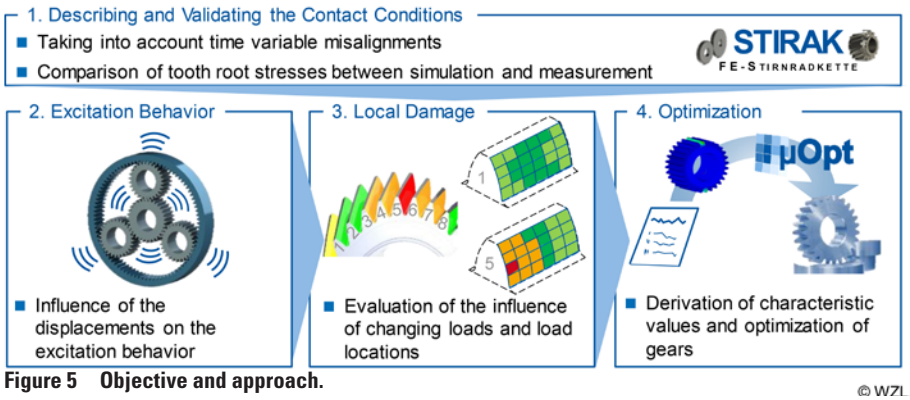

Figure 5 Objective and approach.

discussed to consider misalignments of the planet carrier and the planets in tooth contact (Fig. 7). The calculation of the displacements from internal or external additional forces can be carried out in advance analytically or with the aid of finite element analyses. The method then takes these misalignments into account in the tooth contact analysis and can thus be used to analyze the influence of the respective deviations or for modification design; the method consists of four essential elements.

First, the displacements of the individual shafts are determined in a preceding calculation step. It is possible to use FE calculations or analytical approaches, as well as misalignments acquired by measurement. The input is made via the displacement of the bearing positions. From these, the vectors of the shafts are determined in a common coordinate system for all wheels.

Mathematical operations are used to transform the vectors for each mesh position of a complete tooth hunt on to the tooth contact. For this purpose, the state of the art methods for the transformation of inclination and skew are extended by the kinematics of planetary gears (Ref. 16). The results of this transformation are resultant $f_{H\beta}$ curves for the sun-planet and ring gear-planet mesh.

The resulting curves serve as input variables for the FE Spur Gear Chain → *FE-Stirnradkette*. Deviations from the ideal tooth contact are considered as contact distances in the spring model; a new FE calculation is therefore not necessary, which leads to an optimization of the calculation time and quick evaluation of the results. Loads of the individual gears are determined for each meshing position of a complete tooth hunt. The results of the tooth contact analysis can be post-processed afterwards.

Measurement results of the FVA nacelle. The planet carrier is connected to the rotor of the wind turbine and supported by a main bearing (Fig. 6). The gear housing, in which the remaining gears are mounted, is supported by two flexible mounting points on the torque arm of the main frame. This mounting of the housing enables a tilting of the gear housing due to the weight force in comparison to the planet carrier (Ref. 15).

Due to this effect, there is a misalignment of the planet carrier with respect to the sun and ring gear. The loads on the sun gear are measured in the test gearbox via strain gauges in the tooth root. With the help of the rotation angle measuring systems, the current position of the gears can be determined in a post-processing and thereby at which carrier position the loads occur. The results show that the load distribution varies over the carrier angle due to the misaligned position. This can lead to significant overloads in the tooth contact.

The highest stresses occur in the tooth root if the meshing takes place at an upper 180° or lower position 0°/360°. Between these two positions the location of the maximum stress also changes from the right to the left flank side of the sun gear. The lowest loads and the best load distribution are at the horizontal positions at 90° and 270°, respectively.

Because of the dependence of the contact conditions on the carrier position, the same contact conditions always occur at the fixed ring gear on one tooth, so that this tooth always experiences the same load. On the sun and planet gear, however, the angular position at which a tooth comes into contact varies. This means that every contact position occurs on every tooth during a complete tooth hunt and the tooth load is time-variable. This finally results in internal load spectra already at constant external loads and displacements due to changed contact conditions.

Validation of the extension. In the following section, the calculation approach for the consideration of the carrier misalignments in the tooth contact analysis is validated. Measurement results of the FVA nacelle are used and compared with the results of the simulation method. The tooth root stress of the sun gear and the load distribution factor $K_{F\beta}$ for each position are used as evaluation variables. The load case corresponds to the nominal

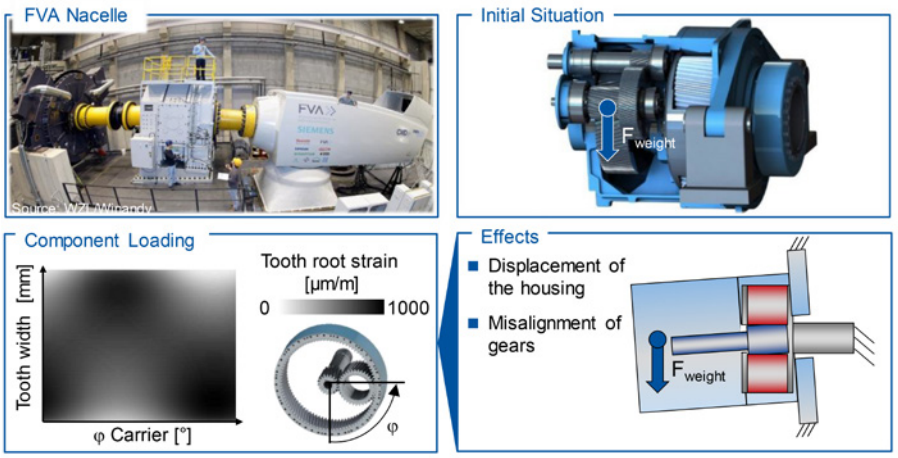

Figure 6 Test setup and occurring effects. © WZL

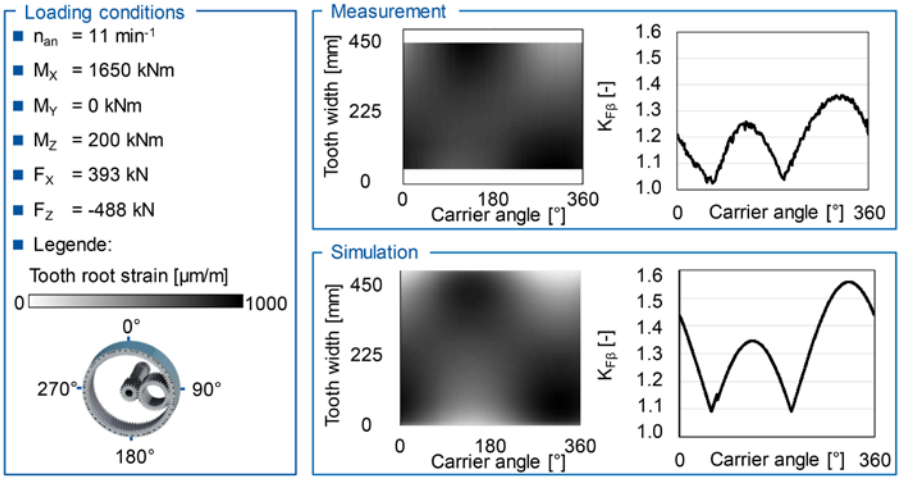

Figure 7 Validation of the simulation method. © WZL

torque of the system with $M_x = 1{,}650$ kNm at an average speed of $n_{in} = 11$ rpm. Further loads applied to the shaft simulate, on the one hand, the rotor weight of the turbine in the direction of F_z and, on the other hand, bending moments and transverse forces from inclined wind flows on the rotor.

The misalignment of the planet carrier measured by distance sensors is used as the input variable of the method. The effects from the planetary axis are not considered in this example, since the influence of these displacements is small compared to the carrier displacement. The maximum values of the resulting $f_{H\beta}$ from the measured misalignment in the sun mesh are $\Delta f_{H\beta} = \pm$ 80 µm; Figure 7 shows the comparison of measurement and simulation.

The measurement results in the load case evaluated here show a clear dependence of the load distribution and the locally occurring tooth root stresses on the current carrier position. As explained previously, the maxima of the load distribution are located at approximately 0° or 360° and 180°. This corresponds to a mesh position in the upper and lower area of the ring gear. The highest load occurs in the tooth mesh in the 0° range. Between the two maxima, a change of the more heavily loaded flank side can also be seen. In the measurement, the width load distribution factor in the tooth root $K_{F\beta}$ shows values between $K_{F\beta} = 1.03$ and $K_{F\beta} = 1.38$, depending on the meshing position. The maximum at approx. 180° has a $K_{F\beta} = 1.25$.

The progression of the tooth root stresses can be correctly predicted with the method — both in width direction and in dependence of the carrier angle. The amplitudes of the stresses are in the same range as in the measurement, and also the location of the maximum load is identical. When comparing the width load factor $K_{F\beta}$ between simulation and measurement, identical characteristics can be determined. Both graphs show maxima at 0° and 180°. The $K_{F\beta}$ of the maximum at 180° in the simulation is at $K_{F\beta} = 1.35$ and represents the load occurring in the measurement well. The second maximum is displayed higher in the simulation. The reason for this is on the one hand, the extended evaluation range in the simulation, because in the measurement, the results cannot be resolved up to the edge area, since no strain gauges were applied there. On the other hand, the differences can be explained by the lack of consideration of the flexible planet shaft, which can reduce the tilting due to the present clearance.

Calculation of the Transmission Error of Misaligned Planetary Gearboxes

The approach for calculating the transmission error of misaligned planetary gears uses the results provided by the previous developed and validated method. As input variable of the tooth contact analysis, one load case with measured misalignments is used. In the further investigations only planet carrier misalignments are taken into account during the investigations, because all other misalignments have a position invariable influence and could be optimized afterwards by lead angle modifications (Fig. 4). The misalignments of the carrier are transformed to the individual meshing planes of each single pitch within one complete tooth hunt using the Wittke method as a function of angular carrier position (Ref. 16).

The result of the tooth contact analysis is the transmission error for one pitch for each angular position. The calculation is carried out separately for the sun and ring gear mesh without consideration of cross influences between those. The results of the individual single pitch calculations are combined into an overall signal in chronologically correct sequence. A consideration of differences in the length of a pitch is that premature and post-mature gear meshes or gear clamps do not take place. The evaluation of the signal is done in frequency domain on the basis of the speed-dependent orders. For this a fast Fourier transform (FFT) of the time signal is carried out. The evaluation takes place individually for each load case.

Figure 8 shows the results of the analysis for a load case at nominal load with a carrier misalignment resulting in an $f_{H\beta}$ deviation of $\Delta f_{H\beta} = 144$ µm, compared to a simulation without carrier displacement. Considering a variable displacement, it can be seen that the rotational orders of the carrier are excited in the sun as well as in the ring gear. On the other hand, sidebands appear around the gear mesh orders. In the ring gear mesh a reduction of the amplitude of the first gear mesh order in comparison to the non-displaced variant is noticeable. The amplitude remains almost unchanged in the sun mesh.

Due to the low speeds of the carrier, the resulting excitations caused by the carrier rotation orders lie in the range below a frequency of $f = 1$ Hz and thus are not in the audible range of the human being. An excitation of these frequencies is nevertheless to be reduced, since tower natural frequencies are excited by the low-frequency vibrations of the transmission, which can lead to a swinging up of the turbine on the tower (Ref. 12).

The changed characteristics of the gear mesh orders can be explained mainly by modulation effects. Low-frequency, superimposed oscillations of the rotational orders lead to modulations and thus to the development of sidebands of higher-frequency oscillations of the gear meshes (Ref. 8). The formation of

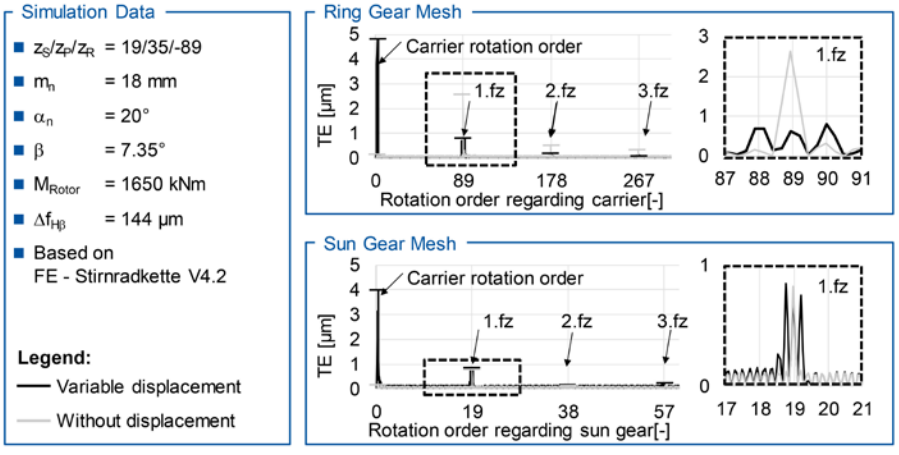

Figure 8 Results of the excitation behavior calculation with and without misalignments. © WZL

sidebands is often aimed for in order to reduce tonalities in the system. In this case, the amplitudes of the sidebands in the sun mesh exceed both, the first order of gear mesh and the amplitude of the undisplaced variant, so that the excitations of the system are amplified.

Influence of Planet Carrier Misalignments on the Load Carrying Capacity

A local accumulation of damage is used to assess the influence of moving contact patterns due to misaligned central elements in planetary gears. The method is similar to the Sfar and Ziegler method, but does not only consider the lower single contact point, but also the complete tooth flank (Refs. 13 and 17). The main difference to the existing methods is the consideration of internal load spectra resulting from shifted central elements with the help of the calculation of a complete tooth hunt. For the load calculation, a method for the analysis of the tooth contact with misaligned central elements developed and validated in the previous section is used. The load capacity is represented by an S/N curve, and sliding velocities are currently not taken into account. In the second part of this section, a comparison of the load carrying capacity of the tooth flanks is carried out with variable, constant and none displaced contact patterns for a load spectra in order to identify the influence of variable misalignments on local damage. Measured displacements of the FVA nacelle are used.

Approach to determine local damage. The previously developed method is extended in the present section so that the determined data can be post-processed in order to calculate the local damage of the tooth flank. In addition, the possibility to consider different external drive torques and misalignments via a load spectra specification is made possible.

In a first step, operating points "*v*" or load bins are specified (Fig. 9, bottom-left). In addition to the drive torque and the percentage of a load bin in the total number of load cycles, the displacement of individual gear elements is another input variable. Possible specifications are, for example, misalignments of the planet carrier, the ring gear or the planet in relation to the sun gear.

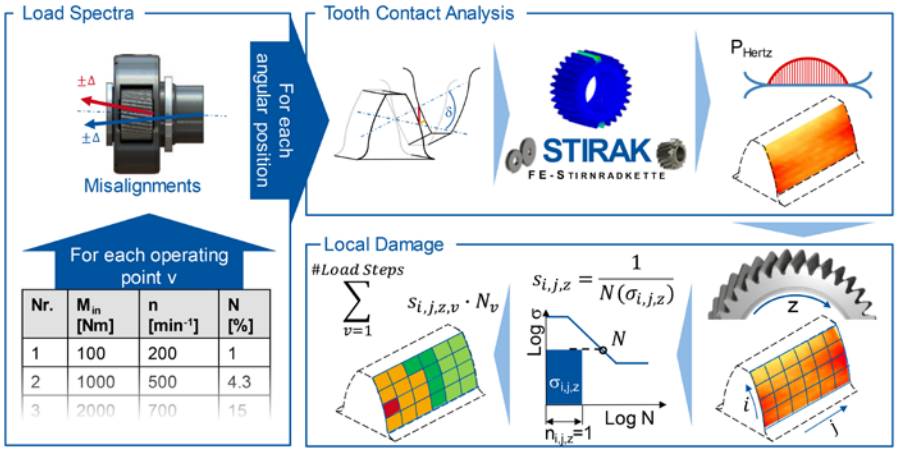

Figure 9 Approach for local damage accumulation. © WZL

Table 1: Overview of regarded load bins

Nr.	Mx [kNm]	My [kNm]	Mz [kNm]	Carrier angle [°]	Load Cycles [%]
1	304	0	0	0.0277	10
2	639	0	0	0.0157	5
3	973	0	0	0.0187	20
4	1312	0	0	0.0170	30
5	1650	0	0	0.0204	20
6	1650	1000	0	0.0065	7
7	1650	-1000	0	0.0157	8

The contact conditions as well as the torque are used individually for each pitch as input data of the FE-based tooth contact analysis *FE-Stirnradkette*. As a result of the tooth contact analysis, the tooth flank pressures according to Hertz are used for the further calculation. The tooth root load capacity is not examined in this report. For this purpose the tooth root stresses would be evaluated instead of the Hertzian pressure and a local accumulation of damage in the tooth root would be carried out.

In order to assess the local damage, the tooth in contact *z* corresponding to the angular position of the gear elements is identified at each gear for each single pitch. Each tooth is additionally rastered in *i* rectangular elements along the height and *j* elements in width direction. For each area of the grid, the maximum pressure is determined when one pitch is rolled over. The occurring flank pressure $\sigma_{i,j,z}$ of each element is the input variable for the evaluation of the individual damage. An S/N curve is used to determine the bearable number of load cycles $N_{i,j,z}$ for the determined pressure $\sigma_{i,j,z}$. The partial damage $s_{i,j,z}$ of an element due to one load cycle is defined as the reciprocal of the bearable number of cycles $N_{i,j,z}$, (Fig. 9, bottom-center).

For each load bin "*v*", a complete tooth hunt is simulated so that all angular positions of the gear elements relative to each other are regarded. This means that several pitches are rolled over and all teeth are in contact several times. A partial damage by an additional contact is added to the already existing damage, so that finally a partial damage of all teeth and all flank elements for a complete tooth hunt of one load bin exists. This value is then divided by the number of pitches calculated for a complete tooth hunt and multiplied by the absolute number of cycles N_v of the load bin. The result is a total damage caused by the individual load bin. It should be noted here that the number of load cycles at the sun gear and ring gear must be multiplied by the number of planets, since the individual flanks are over-rolled several times. The results of the individual load bins are summed up so that a total damage of the individual flank elements results, taking into account the load spectra and corresponding measured misalignments.

Results of the evaluation of local damage. Selected test points together with the corresponding measured carrier misalignment represent the load bins of the investigated load spectrum. This leads

to plausible combinations of torques and misalignments. The internal load spectra result from the carrier displacement. The distribution of the number of load cycles among the respective collective classes does not correspond to reality, but is distributed in such a way that a large part of the operation takes place at nominal torque. An overview of the input data used can be found in Table 1. All operating points show a constant weight force of the rotor in z direction of F_z = - 488 kN, a loading with axial and bending forces F_x and F_y does not occur.

In addition to the loads resulting from the operating conditions, the strength of the material is a necessary input variable for describing the local damage. The material behavior is described by an S/N curve (Fig. 10). The corresponding values for the sun and planetary gears are determined for case-hardened gears from ISO 6336 Part 5 for the material quality MQ (Ref. 5). Values for wrought alloyed material are used for the material behavior of the ring gear. The durable permissible flank pressure of the case-hardened gears is σ_H = 1,300 MPa, of the ring gear σ_H = 520 MPa (Fig. 10, top-center). The consideration of carrier misalignment in the damage accumulation on the flank is carried out in three different ways. In the first variant, as described previously, the misalignment is calculated for each gear mesh on the basis of the angular position of the elements (variable misalignment). In the second variant the misalignment of the carrier is not considered (no misalignment), and in the third variant the maximum occurring value is assumed for all positions (maximum misalignment).

The pressures on the tooth flank calculated from the tooth contact analysis do not correspond to the standard value of the flank pressure σ_H, since application factors are not taken into account. In addition, the load spectrum does not correspond to reality, so that a calculation of the absolute damage value is not conducive. However, a relative comparison of the calculated local damage between individual flank areas or designs is legitimate. Therefore, a normalized damage value $\overline{S_Z}$ is used. This value is defined as the ratio of the maximum damage per tooth $s_{max,lok,z}$ to the maximum damage of a gear $s_{max,lok,var}$ in the calculation with variable displacement.

The upper-right part of Figure 10 shows the results of the local damage accumulation for the planet gear in the sun mesh. It can be seen that the normalized damage assumes a constant value of $\overline{S_Z}$ = 1 for all teeth on the planet gear despite variable misalignment is regarded. The same behavior is observed at the sun gear. At the ring gear, however, different damages occur, depending on the tooth position. Here the tooth at the seventh position is most damaged. The graph shows a maximum at this point, a second local maximum with lower amplitude occurs with 180° offset at tooth 51. The results for the planet gear flank, which is in contact with the ring gear, are not displayed. The pressures occurring are all below the fatigue strength level because of the concave-convex contact, so that no damage can be determined.

The constant damage to the sun and planet gears can be explained by the rotation of the two gears. Each tooth of the sun gear, as well as of the planet gear, does not have a fixed global mesh position; the global position depends on the actual carrier position. The deviations of the gear mesh resulting from the misalignment of the carrier are also dependent on the carrier position; therefore, temporally variable deviations occur at one tooth of the sun and planet gear. After a complete tooth hunt of the planetary gear stage, each tooth of the sun and planet gear are exposed to the same positions and thus to the same loads. Due to the fixed positioning in a load bin, a tooth on the ring gear always has identical mesh conditions. Therefore, the degree of damage changes depending on the tooth position. The second local maximum is smaller, since areas of the tooth flank are stressed in which the supporting effect of the helix angle is missing. As a result, the flank can be deformed better and the pressure values are lower.

The diagrams also show the results of the local accumulation of damage without and with maximum displacement

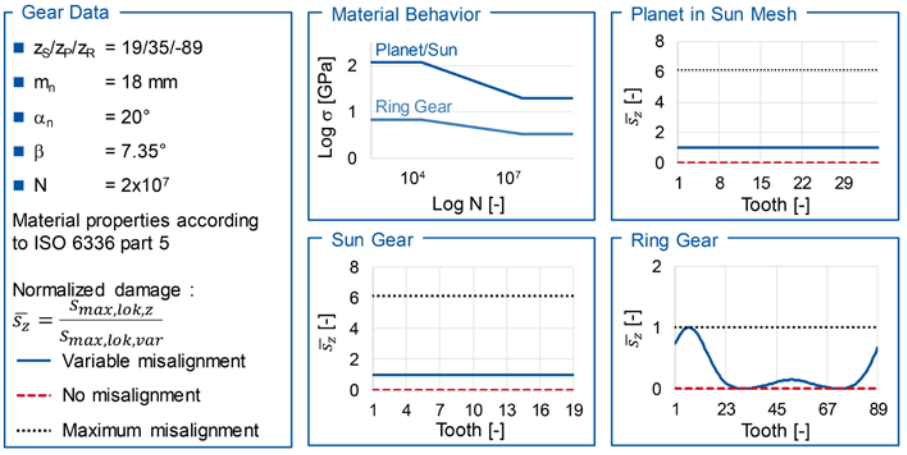

Figure 10 Results of the local damage accumulation. © WZL

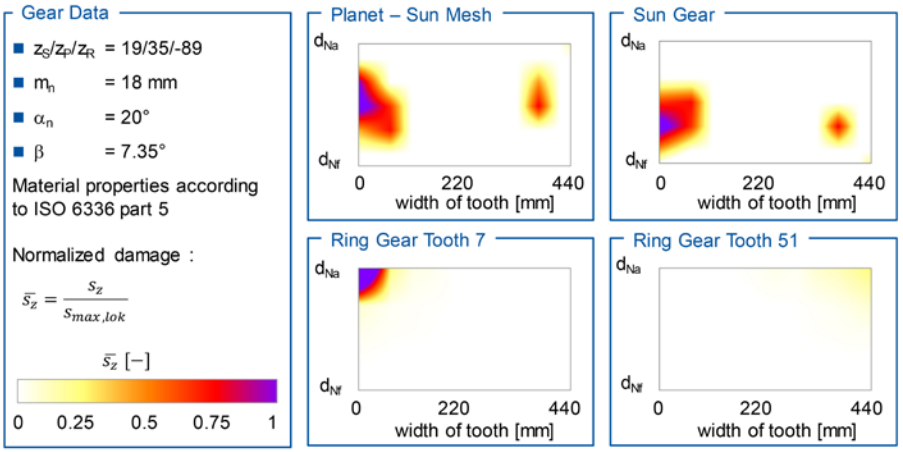

Figure 11 Analysis of the location of local damages. © WZL

(Fig. 10). The locally determined maximum damage with variable displacement was kept as the reference value. It can be determined that no damage to the tooth flanks occurs in a calculation without misalignment. All pressures are below the fatigue strength of the material and are not relevant for damage. If the maximum misalignment is used to assess the damage, the same maximum value is obtained for the ring gear as for the local evaluation. The damage to the sun and planet gear is six times higher than in the local calculation. A dimensioning of the gears with the maximum value of the misalignment would thus be safe, but at the same time clearly over-dimensioned. A dimensioning without consideration of the influence of the variable effects over the circumference, however, leads to under-dimensioned gears.

In Figure 11, the damage values are plotted on the maximum loaded tooth flanks. It can be seen that the damaged areas on all gears are extremely localized. On the planet and sun gear, damaged areas occur on the left and right side of each tooth flank. Here, the left side of the tooth is stressed more than the right side of the flank. The damage to the ring gear depends on the position of the tooth on the circumference; the highest damage is determined at tooth 7. This occurs locally in the tip area on the left side of the flank. At the second local maximum at tooth 51, the right area of the tooth flank is subjected to greater stress. Here, too, the highest damage is found in the tip area, but it is significantly lower than on tip seven.

Due to positive slip, the head areas are generally less relevant to flank damage than high loads in the negative slip area, but nevertheless the local limitation of the damage shows that the flank is used sub-optimally. A uniform damage over the entire flank would correspond to an ideal geometry where all points of the flank fail at the same time. The areas with the highest damage result from edge contact that cannot be robustly compensated by the gear geometry. In the ring gear contact, the maximum stress is located in the area of the upper single contact, since here the highest loads have to be transmitted by a pair of teeth. On the planetary flank there is a tip relief, which reduces the load on the second single meshing area. In sun contact, both single contact areas are relieved due to the tip relief provided on both flanks. This is why the maximum damage occurs in the double-contact area.

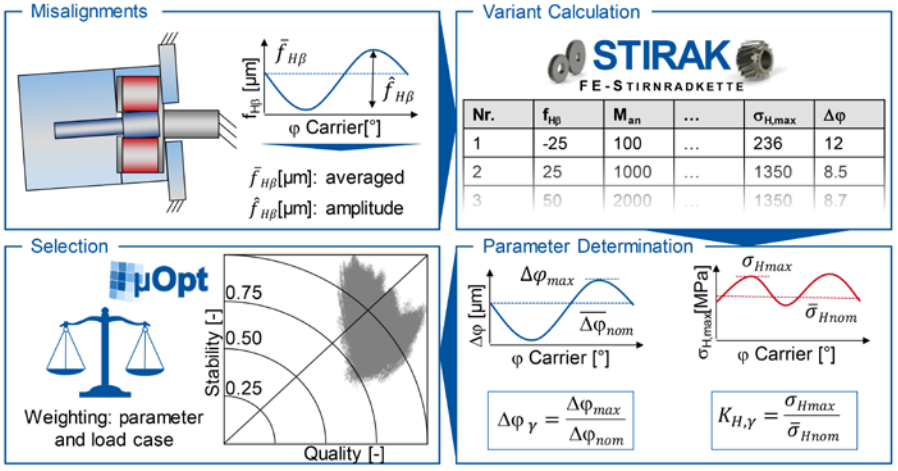

Figure 12 Approach of the design method. © WZL

Optimization of the Operational Behavior of Planetary Gearboxes

The procedure explained here focuses on the design of the flank corrections of the planet. The optimization goal is to increase the robustness of the load carrying capacity against misalignments. In addition, the overall excitation should be reduced — especially in the low-frequency range. As input variables for the design, the averaged lead angle deviation $\bar{f}_{H\beta}$ over one carrier rotation as well as the amplitude of the variation of the lead angle deviation $\hat{f}_{H\beta}$ from maximum to minimum value are taken into account. The design is carried out with a variant calculation in the *FE-Stirnradkette* as well as a post-processing and a statistical evaluation of the results with the help of the *µOpt* program (Fig. 12).

The variant calculation is carried out separately for the individual meshes between sun and planetary gear, as well as ring gear and planetary gear. For this purpose the lead angle deviation is finely resolved over a wide variation range. Using the mean lead angle deviation $\bar{f}_{H\beta}$ and the amplitude of the lead angle deviation $\hat{f}_{H\beta}$ all possible deviations for one nominal design are determined in a post-processing. The individual results of the transmission error and the flank pressure are determined for each lead angle deviation occurring in the misalignment range in one load bin.

From the sum of the individual results, the value $K_{H,\gamma}$ is determined as the factor of the load increase of the tooth flank over one rotation of the carrier and $\Delta_{\phi\gamma}$ as the deviation of the transmission error over one rotation of the carrier for each nominal design and each load step.

For this purpose, the maximum value of the rotational error $\Delta_{\phi max}$ and the flank pressure σ_{Hmax} is determined from all values occurring over one rotation of the carrier and divided by the value occurring for the average $\bar{f}_{H\beta}$. An additional boundary condition, which is added in the evaluation, is the symmetrical design of the flank corrections on both tooth flanks of the planet.

The maximum Hertzian pressure, the transmission error at the average misalignment as well as the two newly introduced load increase factors $K_{H,\gamma}$ and $\Delta_{\phi\gamma}$ are included as parameters in the evaluation of the variants. All values are determined for each nominal variant for the sun and ring gear mesh and then evaluated together. The evaluation takes place depending on the load case and the parameter with the help of the *µOpt* software. Here the load cases are weighted more strongly with increasing rotor torque and the pressure is evaluated higher than the transmission error. The overview of the individual variables is shown (Fig. 13).

The optimized flank geometry essentially differs from the nominal design by an applied profile angle correction and a higher lead crowning. Due to the positive profile angle correction at the planet, the tooth tip of the ring gear is relieved and the area of maximum load moves in the direction of the tooth center. The effect of the changed microgeometry becomes clear when comparing the results of local

damage accumulation before and after optimization. The damage values of the new design are determined and divided by the reference value. The reference value of the normalized damage is the value $s_{max,lok,origin}$ of the original variant.

In the sun mesh, a reduction of the damage can be achieved to a value of X = 0.75 — both at the planet and at the sun gear. The flank damage of the ring gear can be reduced to a value close to $S_z = 0$. The difference between the level of damage depending on the tooth position at the ring gear is also reduced. The reason for this is, on the one hand, the avoidance of edge contacts which have led to high loads in the edge area of the gear teeth. This resulted in high damage values in the original design. On the other hand, the contact pattern in the ring gear mesh moves in the direction of the flank center due to the profile angle correction, whereby locally high pressures in the tip area can be avoided.

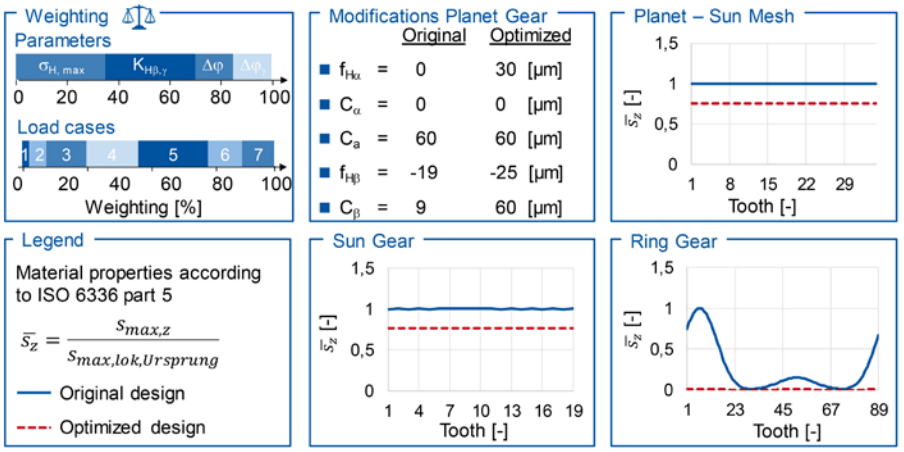

Figure 13 Influence of the optimization on the local damage. © WZL

Summary and Outlook

This study deals with the modeling and consideration of misalignments in planetary gearboxes in the optimization and design process. Procedures for taking into account misalignments in cylindrical gearboxes are standardized and established in industry. Misalignments of central elements like carrier, sun gear or ring gear in planetary gearboxes, cause-varying contact positions and variable loads, depending on the angular position of the central elements. This load, which is variable over the circumference, is not taken into account in the standardized procedures, despite its effects on the loads on the gears.

Within the scope of this report, a method is developed in order to regard carrier misalignments in the tooth contact analysis *FE-Stirnradkette*. Because of carrier position-dependent mesh conditions, a complete tooth hunt is calculated and post-processed afterwards. By means of a comparison between simulated and measured tooth root stresses of the FVA nacelle, a validation of the method is successfully carried out.

By means of the validated method, the influence of carrier misalignments on the load carrying capacity and excitation behavior are determined. In a post-processing of the previously developed method, the transmission error of the single meshes, as well as the damage locally resolved on the tooth flank of each tooth of each gear, is calculated. The transmission error of misaligned and aligned planetary gearboxes differs. In misaligned conditions, sidebands of the tooth mesh frequencies occur. Furthermore, the carrier rotational frequency is excited.

The results of the local damage calculation show that due to the rotation of the sun and planet gear, changing meshing conditions are present on a tooth. In sum, each tooth on these wheels sees the same loads, resulting in homogeneous damage over the wheel. One tooth is always subjected to the same load on the fixed ring gear. This results in variable damage over the circumference, with some teeth being much more damaged than others. If the misalignment of the carrier is not taken into account, the wheels will not be damaged at all. If the maximum misalignment is assumed in all positions, too high damage is calculated, except for the ring gear.

The optimization is carried out via the flank corrections on the planetary gear. For this purpose the deviation range, as well as the mean value of the resulting lead angle deviation, are included in the calculation in order to take the misalignment of the carrier into account. New characteristic values are generated for the consideration of the load increase over the circumference $K_{H\gamma}$ as well as the deviation range of the transmission error over the circumference $\Delta_{\phi\gamma,}$ and different nominal designs are compared with the help of the *µOpt* software. The recalculation of the best variant shows a reduced damage of all flanks, despite a higher crowning. The effect of the varying damage over the ring gear circumference can almost be eliminated.

As a next step, slippage effects will be regarded during the local damage calculation to better predict the localization of failure. Also measurements will be done on a smaller test rig to validate the effects observed in the evaluation of the excitation behavior. Therefore, different distinct misaligned conditions can be set and the transmission error can be measured.

Power Transmission Engineering (FVA) for the software *FE-Stirnradkette*. The authors gratefully acknowledge support by the WZL Gear Research Circle for the software *µOpt*. The authors gratefully acknowledge financial support by the Federal Ministry for Economic Affairs and Energy (FKZ 0325799) for the achievement of the project results.

For more information.

Questions or comments regarding this paper? Contact Julian Theling at *kj.theling@wzl.rwth-aachen.de*.

References

1. Bastert, C.-C. "Die Verlagerung der Zentralräder in Planetengetrieben." In: Forsch Ing-Wes, 37. Jg., 1971, Nr. 1, S. 21–29.
2. Brecher, C., C. Löpenhaus and D. Piel. "Auslegung und Untersuchung eines Forschungsgetriebes für Windkraftanlagen mit der FE-basierten Zahnkontaktanalyse DMK," Dresden: TUD press, 2015.
3. Brecher, C., C. Löpenhaus, J. Theling, M. Schroers and D. Piel. "FE-Based Method for Design of Robust Tooth Flank Modifications for Cylindrical and Planetary Gear Stages Regarding Manufacturing Tolerances," *AGMA Fall Technical Meeting,* 2017.
4. Ingeli, J. "Erweiterung der FE-basierten Zahnkontaktanalyse zur normkonformen Grübchentragfähigkeitsberechnung symmetrischer und asymmetrischer Verzahnungen," Dissertation IIF - Institut für Industriekommunikation und Fachmedien GmbH, 2017.
5. ISO 6336 Teil 5. (Juli 2003) Calculation of load capacity of spur and helical gears, Strength and Quality Materials.
6. ISO 6336 Teil 3. (September 2006) Calculation of load capacity of spur and helical gears, Calculation of Tooth Bending Strength.
7. ISO06b ISO 6336 Teil 2. (September 2006) Calculation of load capacity of spur and helical gears, Calculation of Surface Durability (Pitting).
8. Landvogt, A. "Einfluss der Hartfeinbearbeitung und der Flankentopographieauslegung auf das Lauf- und Geräuschverhalten von Hypoidverzahnungen mit bogenförmiger Flankenlinie," Diss. RWTH Aachen University, 2003.
9. Lubenow, K., F. Schuhmann and S. Schemmert. *Requirements for Wind Turbine Gearboxes with Increased Torque Density with Special Attention to a Low-Noise Turbine Operation,Conference for Wind Power Drives* 2019, Norderstedt: Books on Demand, 2019.
10. Miner, M. "Cumulative Damage in Fatigue," *Journal of Applied Mechanics-Transactions of the ASME*, 12. Jg., 1945, Nr. 3, S. A159-A164.
11. Niemann, G. and H. Winter. *Maschinenelemente. Band 2: Getriebe allgemein, Zahnradgetriebe - Grundlagen, Stirnradgetriebe*. Bd. Nr. 2, 2. Aufl. Berlin: Springer, 2003.
12. Seidel, M. "Auslegung von Hybridtürmen für Windenergieanlagen - Lastermittlung und Nachweis der Ermüdungsfestigkeit am Beispiel einer 3,6-MW-WEA mit 100 m Rotordurchmesser," *Beton- und Stahlbetonbau*, 97. Jg., 2002, Nr. 11, S. 564–575.
13. Sfar, M. "Bestimmung von Verzahnungskorrekturen und Lagerkräften in Planetengetrieben für Lastkollektive," Diss. Ruhr-Universität Bochum, 2011.
14. Theling, J., C. Brecher and C. Löpenhaus. "Einfluss von Planetenträgerabweichungen auf die Lokale Lastverteilung in Planetengetrieben," KISSsoft AG (Hrsg.): SMK 2018. Dresden: TUD press, 2018.
15. Vriesen, J. "Berechnung der Verzahnungskorrekturen von Planetenradgetrieben unter Berücksichtigung der Steg- und Hohlradverformungen," Diss. Ruhr-Universität Bochum, 2001.
16. Wittke, W. "Beanspruchungsgerechte und Geräuschoptimierte Strinradgetriebe Toleranzvorgaben und Flankenkorrekturen," Diss. RWTH Aachen University, 1994.
17. Ziegler, A. "Zur verkürzten Systemlebensdauerprüfung von Zahnradgetrieben," 1, Aufl. Aufl. München: Verl. Dr. Hut, 2011.

Prof. Dr.-Ing. Christian Brecher has since January 2004 been Ordinary Professor for Machine Tools at the Laboratory for Machine Tools and Production Engineering (WZL) of the RWTH Aachen, as well as Director of the Department for Production Machines at the Fraunhofer Institute for Production Technology IPT. Upon finishing his academic studies in mechanical engineering, Brecher started his professional career first as a research assistant and later as team leader in the department for machine investigation and evaluation at the WZL. From 1999 to April 2001, he was responsible for the department of machine tools in his capacity as a Senior Engineer. After a short spell as a consultant in the aviation industry, Professor Brecher was appointed in August 2001 as the Director for Development at the DS Technologie Werkzeugmaschinenbau GmbH, Mönchengladbach, where he was responsible for construction and development until December 2003. Brecher has received numerous honors and awards, including the Springorum Commemorative Coin; the Borchers Medal of the RWTH Aachen; the Scholarship Award of the Association of German Tool Manufacturers (Verein Deutscher Werkzeugmaschinenfabriken VDW); and the Otto Kienzle Memorial Coin of the Scientific Society for Production Technology (Wissenschaftliche Gesellschaft für Produktionstechnik WGP).

Dr. -Ing. Dipl. -Wirt. -Ing. Christoph Löpenhaus has since 2014 served as Chief Engineer in the Gear Department of WZL, RWTH Aachen / Laboratory of Machine Tools and Production Engineering (WZL), RWTH Aachen. He previously held positions there as (2011–2014) Team Leader, Group Gear Testing Gear Department Chair of Machine Tools Laboratory of Machine Tools and Production Engineering (WZL) RWTH Aachen; (2010–2011) Research Assistant, Group Gear Testing Gear Department Chair of Machine Tools Laboratory of Machine Tools and Production Engineering (WZL) RWTH Aachen: (2007–2009) as Student Researcher, Group Gear Design and Manufacturing Calculation Gear Department Chair of Machine Tools Laboratory of Machine Tools and Production Engineering (WZL) RWTH Aachen; and (2004–2009) as a student in Industrial Engineering RWTH Aachen.

Since June 2019 **Julian Theling M.Sc**. has been the leader of the Gear Acoustics group at the Laboratory of Machine Tools and Production Engineering (WZL). He started his career as a researcher at the WZL in 2016 after receiving his master's degree in mechanical engineering from RWTH Aachen University. Theling's research focus is the influence of flexible surroundings on the application behavior of planetary gear stages.

For Related Articles Search
planetary gears
at www.geartechnology.com